

PCCP

Accepted Manuscript



This is an *Accepted Manuscript*, which has been through the Royal Society of Chemistry peer review process and has been accepted for publication.

Accepted Manuscripts are published online shortly after acceptance, before technical editing, formatting and proof reading. Using this free service, authors can make their results available to the community, in citable form, before we publish the edited article. We will replace this *Accepted Manuscript* with the edited and formatted *Advance Article* as soon as it is available.

You can find more information about *Accepted Manuscripts* in the [Information for Authors](#).

Please note that technical editing may introduce minor changes to the text and/or graphics, which may alter content. The journal's standard [Terms & Conditions](#) and the [Ethical guidelines](#) still apply. In no event shall the Royal Society of Chemistry be held responsible for any errors or omissions in this *Accepted Manuscript* or any consequences arising from the use of any information it contains.

Modelling Bio-Electrosynthesis in a Reverse Microbial Fuel Cell to Produce Acetate from CO₂ and H₂O

M. Kazemi¹, D. Biria^{1*}, H. Rismani-Yazdi²

1: Department of Biotechnology, Faculty of Advanced Sciences and Technologies, University of Isfahan, Isfahan, Iran

2: Novozymes North America Inc., PO BOX 576, Franklinton, NC 27525 USA

Abstract

Bio-electrosynthesis is one of the significant developments in reverse microbial fuel cell technology which is potentially capable of creating organic compounds through combining CO₂ with H₂O. Accordingly, the main objective in the current study was to present a model of microbial electrosynthesis for producing organic compounds (Acetate) based on direct conduction of electrons in biofilms. The proposed model enjoys a high degree of rigor because it can predict variations in the substrate concentration, electrical potential, current density and the thickness of biofilm. Additionally, coulombic efficiency was investigated as a function of substrate concentration and cathode potential. For a system containing CO₂ as the substrate and *Sporomusa ovata* as the biofilm forming microorganism, an increase in the substrate concentration at a constant potential can lead to a decrease in coulombic efficiency as well as an increase in current density and biofilm thickness. On the other hand, an increase in the surface cathodic voltage at a constant substrate concentration may result in an increase in the coulombic efficiency and a decrease in the current density. The maximum coulombic efficiency was revealed to be 75% in the substrate concentration of 0.025 mmol cm⁻³ and 55% in the surface cathodic voltage of -0.3 V producing a high range of acetate production by creating an optimal state in the concentration and potential intervals. Finally, the validity of the model was verified by comparing the obtained results with related experimental findings.

Keywords: Electrosynthesis, Reverse Microbial Fuel Cell, Modelling, Coulombic Efficiency, Acetate, Biofilm

* Corresponding to Davoud Biria, E-mail: d.biria@ast.ui.ac.ir, Tel: +98-31 37934373

1. Introduction

One of the most exciting applications of microbial interactions with electrochemistry is microbial electrosynthesis (MES). In fact, the process can be defined as an artificial form of photosynthesis in which microorganisms utilize electrons derived from an electrode to reduce carbon dioxide and water to multi-carbon extracellular products and oxygen [1]. Electrosynthesis could be considered as an effective strategy to store the electrical energy from renewable solar or wind sources in form of chemical structures. The production of liquid transportation fuels with MES is particularly attractive because the electricity generation by renewable technologies is neither continuous nor always compatible with demand and its storage is quite difficult. Large-scale fuel production could readily convert electrical energy into covalent carbon bonds permitting storage and delivery upon demand within existing infrastructure [2, 3].

Reaction thermodynamics suggests that it is readily feasible to reduce carbon dioxide electrochemically to a diversity of organic compounds, and this process has been studied for over a hundred years [4]. Practically, the main criteria for an electrochemical system of carbon dioxide fixation are (i) the capability of using electrons derived from water as an abundant, inexpensive source of reductant; and (ii) the existence of an inexpensive, durable catalyst [5, 6, 7]. Therefore, adequate electrocatalysts are needed to forward the electrode-driven chemical reactions in electrosynthesis. Accordingly, the application of biocatalysts has been gradually increased in electrosynthetic processes because of their higher specificity and versatility relative to existing chemical catalysts. Generally, bioelectrosynthesis relies on the interaction between biocatalysts and electrodes and mainly employs immobilized enzymes or organelles on the electrode surfaces [4, 6, 8, 9]. Recently, MES has been introduced to describe the electricity-driven reduction of CO₂ using the whole microorganisms as electrocatalysts [4, 10].

Most of the successful applications of microbe electrode interactions for bioelectrosynthesis have been reported in reverse microbial fuel cells (R-MFCs) which are based on direct suppliance of electrons to microorganisms at the cathode surface to activate the biocatalysis process [8]. Microbes in the cathodic chamber consume electrons to reduce the substrate molecules, and generate the final products of the process [11]. In addition, the energetics of the living system is provided by the electron transfer process [12, 13, 14].

Several microorganisms (e.g., *Sporomusa ovata*, *Clostridium ljungdahlii*, *Clostridium aceticum*, and *Moorella thermoacetica*) have been identified which can grow on CO₂ as the electron acceptor and reduce it into organic chemicals through an anaerobic respiration process [12, 13]. Among them, acetogenic microorganisms are strict anaerobic bacteria that can couple H₂O oxidation with CO₂ reduction to produce acetate [12, 13]. The capability of acetogenic bacteria such as *Sporomusa ovata* in acquiring electrons from graphite electrodes to reduce carbon dioxide to acetate has proved the possibility of bioelectrosynthesis concept. It was reported that *S. ovata* biofilm on the electrode surface of a R-MFC system can produce acetate as well as small amounts of 2-oxobutyrate concomitantly with current consumption so that the electron recovery for these products may be over 85% [10]. Substantial acetate production has been reported in recent R-MFC or MES studies [12, 13, 14].

Although the microbial electrosynthesis in a R-MFC system is a nascent concept, its performance can be predicted by modeling the process through the specific mechanisms for electron transfer and chemicals/biofilm interactions. To this end, the present paper aims at modeling the MES in the cathodic chamber of R-MFC system. In addition, the validity of the proposed model will be verified by relevant experimental results concerning the system.

2. Model description

The primary goal for modeling a MES in a R-MFC system can be considered as estimating the electrical energy consumption and production of the desired chemicals. The electrical current will be consumed when certain dissolved chemical species are reduced and biomass is produced on the cathode. Therefore, the first task is to define rate equations for consumption of substrate, growth of microorganisms, self-oxidation of active microorganisms and their inactivation. Secondly, it is necessary to describe biofilm model using mass balances of the substrate in biofilm and the liquid catholyte because the concentrations of chemical and biomass components are influenced by the mass transfer and reactions in the biofilm and the bulk liquid. Then, the estimation of ohmic resistances is required to calculate the electrical current using electrical potential equation and Ohm's law. Finally, minimum amounts of substrate concentration and electrical potential could be calculated.

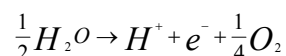
In this work, the final model was implemented as a computer code in MATLAB software package. All of the soluble components and biomass type with their relevant physical, chemical and biological attributes were thoroughly defined. Electrochemical and (bio) chemical reactions were also defined based on their stoichiometry and rate parameters.

The proposed model here is applied for the particular case of a R-MFC fed with carbon dioxide working in a continuous mode operation by considering the following assumptions:

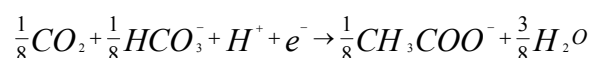
- Electrons current supplies with an external source
- Unsteady-state and one-dimensional system has been assumed to describe biofilm growth and decay
- Electrons transfer based on an electrical conduction mechanism through the conductive biofilm

- Diffusion coefficient of the substrate in the biofilm is equal to 79% of its diffusion coefficient in the aqueous phase
- Concentration profiles in the concentration boundary layer adjacent to the biofilm has been assumed to be linear
- Intracellular processes in the electron transfer have been neglected
- Detachment of microorganisms has been ignored in determination of the biofilm thickness
- A cylindrical geometry has been Considered for the cathode
- The electrical resistances of electrodes and the ion exchange membrane have been neglected
- pH assumed to be constant in the biofilm and electrolyte
- The overall reactions in the system has been assumed as follows:

Half reaction in the anode:



Half reaction in the cathode:



The employed terms for Model parameters have been shown in table 1.

2.1. Bioaction Kinetic Equations

2.1.1. Substrate Consumption Rate

Concentration of electron acceptors plays an important role in determination of biological processes rate. Microbial biofilm receives electrons from anode and delivers them to carbon dioxide as the final electron acceptor [10]. Monod equation was used to describe the kinetics of

bacterial growth in the system [10]. Since the bacterial growth directly relates to the substrate consumption rate the same equation can be used to explain the dependency of substrate consumption rate to its concentration. The equation has been shown below:

$$q = q_{max} \phi_a \frac{S_d}{S_d + K_{sd}} \quad (1)$$

In the cathodic chamber of R-MFC, the amounts of both conductive biofilm as the electron donor and substrate (carbon dioxide) as the electron acceptor affect the electrosynthesis kinetics significantly. In fact, the concentrations of electron donor and electron receptor can restrict the substrate consumption rate. Therefore, the above equation should be modified in the form of equation 2 below to consider the limiting effects of electron donor and electron acceptor at the same time [12, 13]:

$$q = q_{max} \phi_a \frac{S_d}{S_d + K_{sd}} \frac{S_a}{S_a + K_{sa}} \quad (2)$$

However, the expression of concentration for an electrically conductive biofilm, seems to be meaningless and the impact of biofilm as the electron acceptor should be described differently. Consequently, the electrical potential has been employed to explain the electron acceptor role of the biofilm because it is the main driving force for transporting electrons in a conductive medium [15]. Accordingly, the final form of the substrate consumption rate equation will be stated in form of equation 3:

$$q = q_{max} \phi_a \left(\frac{1}{1 + \exp\left(\frac{-F}{RT} \eta\right)} \right) \left(\frac{S_a}{S_a + K_{sa}} \right) \quad (3)$$

In this equation, $\eta = E_{KA} - E_{cathode}$, indicates the electrical potential in various parts of the cathodic biofilm toward E_{KA} (V). E_{KA} is the potential in which the substrate consumption rate will reach to half of the maximum substrate consumption rate [15].

2.1.2. Self-Oxidation Rate of Active Microorganisms

Microorganisms oxidize a substrate to acquire energy for their maintenance and duplication. In this process, a part of the produced electrons will first transfer to the final electron acceptor to supply cells with the required energy for maintenance (energy producing electrons). Then, the remaining electrons will be consumed to produce new microbial cells (cell generative electrons) [10].

In a R-MFC, energy producing electrons are a part of those transferred from the anode to the final electron acceptor in the cathode to form the final product (e.g. acetate). The function of the remaining electrons is cell generation through duplication of microorganisms to produce new active cells which serve as the biocatalyst in the synthesis process. The bacterial cells will be destroyed either to supply energy requirements for the other active cells in the biofilm or at the end of their natural active life. Therefore, a portion of the consumed electrons in cell generation will be recovered and transferred to the electron acceptor to produce more energy (self-oxidation phenomenon). It should be noted that all of the demolished cells would not be oxidized to produce energy and a part of them would accumulate as inactive, neutralized cells in the biofilm structure [10]. Figure 1 shows a schematic of the consuming routes for the produced electrons by an external source.

The equation of self-oxidation rate of active microorganisms can be expressed as follows [15]:

$$r_{res} = b_{res}\phi_a \frac{1}{1 + \exp\left(\frac{-F}{RT}\eta\right)} \quad (4)$$

2.2. Substrate Mass Balance in Biofilm

The dissolved substrate in the catholyte of the R-MFC must diffuse into the matrix of the biofilm to be oxidized by the active bacteria. The biofilm can be considered as a porous medium and its influence on the substrate diffusion should be taken into account. Therefore, Permeability

coefficient within the biofilm is a function of the biofilm density. Since the substrate mass transfer from the solution to the biofilm and the cathode undergoes mainly through the diffusion mechanism, Fick's law can be employed to describe the phenomenon. Biofilm resistance against diffusion of substrate can be expressed through a 20% reduction in diffusion coefficient of the substrate in water [16]. Moreover, the rate of substrate utilization by the active bacteria in the biofilm has been shown in equation 3 which can be combined with the diffusion forming an equation for the mass balance in the biofilm (equation 5). In this equation the diffusion of substrate into biofilm has been considered as the rate limiting step which means that all of the diffused substrate in the biofilm will be converted to products by the bacteria [12, 17].

$$D_{ED,f} \frac{d^2 S_a}{dz^2} - X_{f,a} q = 0 \quad (5)$$

Figure 2 shows a simple schematic of the process. In this figure, biofilm attaches to the cathode and the concentration boundary layer is located near the biofilm.

Two boundary conditions are needed to solve the above equation. The first one can be readily provided by the fact that the cathode electrode surface is impermeable to the substrate, so the substrate molar flux at this boundary will be equal to zero.

The second condition can be obtained by considering the equality of the substrate molar flux at the biofilm surface with its molar flux through the liquid phase boundary layer. In fact, substrate molar flux passing through the entire biofilm/liquid interface is the same because there are no reactions in the liquid phase boundary layer. Accordingly, boundary conditions for equation (5) can be stated as below:

$$@ z = 0 \quad , \quad \frac{dS_a}{dz} = 0 \quad (6)$$

$$@ z = L_f , D_{ED,f} \frac{dS_a}{dz} = \left(\frac{D_{ED,l}}{L} \right) (S_{a,bulk} - S_{a,surface}) \quad (7)$$

The substrate molar flux in the liquid boundary layer (equation 7) has been described by the film theory where the variations of concentration in the boundary layer thickness are assumed to be linear. Film density near the biofilm causes substrate transfer resistance from bulk liquid to the biofilm surface which in turn leads to a concentration gradient between the aqueous phase and the biofilm. In addition, the internal mass transfer resistance is determined by the porous biofilm resistance against penetration of substrates and its consumption in the bio-electrochemical reaction [18].

In contrast to this assumption, previous research has shown that the concentration profile is non-linear in the vicinity of the biofilm because of the biofilm heterogeneous surface and the influence of the fluid velocity field at that area [19, 20]. Therefore, it is necessary to consider these effects in equation 7 to predict mass transfer coefficients properly.

2.3. Investigation of External Mass Transfer Coefficient

The existence of concentration boundary layer in the vicinity of the biofilm causes an external mass transfer resistance which makes the substrate concentration at the biofilm surface to be lower than its concentration in the bulk liquid of the catholyte. The thickness of this layer is variable according to the physical properties of the flow and the velocity field. In addition, the magnitude of the mass transfer resistance created by the boundary layer is a direct function of the layer thickness. Consequently, estimating the mass transfer coefficient in the concentration boundary layer is necessary in order to evaluate conditions in the continuous flow mode. It should be noted that the film theory can be used unchanged in the batch mode (equation 7) when there is no fluid flow in the system.

In order to determine the effect of flow field and its average velocity on the external mass transfer coefficient, the formulas can be presented in terms of dimensionless numbers [21, 22, 23]:

$$Sh = 2 Re^{0.5} Sc^{0.5} \left(\frac{d_h}{L}\right)^{0.5} (1 + 0.0021 Re) \quad (8)$$

$$k_l = Sh \frac{D_{ED,l}}{d_h} \quad (9)$$

$$Re = \frac{\bar{u} d_h}{\nu} \quad (10)$$

$$Sc = \frac{\nu}{D_{ED,l}} \quad (11)$$

To calculate the substrate concentration profile in the biofilm, the external mass transfer resistance should be modeled by the Film theory through equation 9 and 10 [23]. Then, the internal mass transfer resistance is determined by calculating the porous biofilm resistance against penetration of substrates which can be estimated as a rule of thumb by about 20% reduction of the diffusion coefficient in water. Finally, the obtained Mass transfer coefficient from equation 9 can be inserted in equation 7 as a substitute of $\frac{D_{ED,L}}{L}$.

2.4. Substrate Mass Balance in the Catholyte

In the equation 7, the substrate concentration in the catholyte solution has been considered to be constant. Constant concentration of the substrate in the catholyte can be achieved in the final state of the continuous flow (steady state). Assuming plug flow in cathodic chamber, the variation of substrate concentration in the bulk liquid volume with time and cathode length can be described by a non-steady equation:

$$V_{c,b} \left(\frac{\partial S_{a,bulk}}{\partial t} + u_x \frac{\partial S_{a,bulk}}{\partial z} \right) = -A_s J_s \quad (12)$$

The initial and boundary conditions for this equation can also be expressed as follows:

$$@ t = 0 \quad , \quad S_{a,bulk} = S_{a,bulk}^0 \quad (13a)$$

$$@ z = 0 \quad , \quad S_{a,bulk} = S_{a,in} \quad (13b)$$

2.5. Electrical Potential Equation and Ohm's Law

In the present model, it has been assumed that the transfer of electrons is controlled by electrical conductivity of the biofilm. Thus, the biofilm on the cathode surface has been considered as an Ohmic conductor. The equation 14 shows this assumption [24]:

$$j = -\kappa_{bio} \frac{d\eta}{dz} \quad (14)$$

Similar to the process of deriving the equation of substrate mass conservation in the cathode (equation 5), the conservation of electrons should be presented in this section. Consequently, the electric potential equation in the cathode can be considered as equation 15 [25]:

$$\kappa_{bio} \frac{d^2\eta}{dz^2} - \frac{F \gamma_1}{\tau} f_e^0 X_{f,a} q + \frac{F \gamma_2}{\tau} X_{f,a} r_{res} = 0 \quad (15)$$

The first term in the equation 15 represents electron conduction through the conductive biofilm with electrical conductivity coefficient, κ_{bio} , and electrical potential η which are transferred from the cathode to the outer surface of bacteria. The second and third terms illustrate the electron consumption and the electron generation in the system, respectively.

There are two remarkable points about equation 15. Firstly, the consumption of electrons for synthesis of the final product: this is the most important way of the electrons consumption, which is depicted by the second term of equation 16. Each mole of the substrate is consumed by the rate

of $X_{f,a} \cdot q$ and converts to the product with γ_1 electrons. Only the f_e^0 fraction of incoming electrons in the cathode goes to product and the remaining fraction will be allocated to cell duplication and generation of new biomass. The molar value of electrons ($f_e^0 \gamma_1 X_{f,a} \cdot q$) is converted to the electric charge through the Faraday's constant, F . Secondly, generated electrons current from self-oxidation of active microorganisms: this part of the generated electrons, which is illustrated by the third term of equation 15, forms a trifle quota of input electrical current. Every mg of active microbes is oxidized with $X_{f,a} \cdot r_{res}$ rate and produces γ_2 mole electrons which is converted to the electric charge through the Faraday's constant. The amount of γ_2 is calculated by assumption of $C_5H_7O_2N$ formula for active microorganisms in the biofilm and also N_2 as nitrogen resource of bacteria [10].

The produced electrons in the biofilm cannot be transferred and conducted into the catholyte liquid. Therefore, the electrical load flux must be zero at the interface of the biofilm and liquid solution. As a result, one of the boundary conditions for equation 15 will be acquired as:

$$@ z = L_f \quad , \quad \frac{d\eta}{dz} = 0 \quad (16)$$

To derive the second boundary condition for equation 15 two different cases can be considered:

1- The cathode surface potential has been fixed by Potentiostat:

$$@ z = 0 \quad , \quad \eta = E_{KA} - V_{cathode} \quad (17)$$

2- The cathode surface potential changes due to connection to an external source of electrons and external electrical resistances:

$$@ z = 0 \quad , \quad \eta - \left(A_s \cdot \kappa_{bio} \cdot \sum R \right) \frac{d\eta}{dz} = E_{KA} - V_s \quad (18)$$

Generally, all of the resistances in the fuel cell against the transfer and movement of electrically charged species are Ohmic resistances with two main types: i) Resistance of

electrolyte solution and the ion exchange membrane against the transfer of ions, and ii) the biofilm and electrodes resistance to transfer of electrons. The Ohmic resistance of electrodes can be neglected because they are usually made of materials with high electrical conductivity such as graphite, carbon and metals. The effect of cation exchange membrane (Nafion) on the ohmic resistance and produced power density by a microbial fuel cell has been previously examined [26]. The results indicated that the presence of cation exchange membrane Nafion did not have a significant effect on reduction of the produced power density. Thus, the membrane resistance against ion transfer can also be ignored by assuming the presence of a Nafion 117 membrane in the model, which has been frequently used in many fuel cells.

Accordingly, it can be said that the main factors in the ohmic resistances generated in the reverse microbial fuel cells are cathodic biofilm and electrolyte solution. The biofilm resistance is determined by its electrical conductivity coefficient (K_{bio}). The resistance of the electrolyte solution against ions transfer, and consequently, the amount of generated voltage drop can be calculated by the equation 20 [25, 27]:

$$\Delta V_{ohm} = \frac{d \cdot j}{\kappa_{sol}} \quad (19)$$

In this equation, voltage drop due to the resistance of the electrolyte solution is determined in terms of electrical conductivity coefficient and distance of electrodes from ion-exchange membrane. This equation can be utilized in the equation 18. Distancing of electrode from membrane is involved in determining of ΔV_{ohm} because cations from decomposition of the water molecules in the anode must traverse a pass after the membrane to the cathodic chamber to reach the biofilm attached to the cathode electrode.

2.6. Mass Conservation for the Biofilm

A portion of the viable bacteria will be inactivated in the biofilm and form a neutral population. The inactivation rate can be expressed as follows [15]:

$$r_{ina} = b_{ina}\phi_a \quad (20)$$

In this equation, the inactivation rate will be more significant in the higher number active microorganisms.

The viable microbial species generally act as biocatalysts which facilitate the electron transfer to carbon dioxide as the substrate and its conversion to the final product. Naturally, the active cells are alive which will be converted to neutral and inactive species after completing their life span. While the neutral species can conduct the electrical current, they have no catalytic role in substrate conversion to the product. In the other words, the inactive species just fill a portion of the biofilm space.

The conservation of mass equation for the active microbial cells has been expressed below [11]:

$$\frac{\partial \phi_a}{\partial t} + \frac{\partial(v \phi_a)}{\partial z} = Yq - r_{res} - r_{ina} \quad (21)$$

Inactive microbes are generated with a specific rate (r_{ina}) according to the following equation:

$$\frac{\partial \phi_a}{\partial t} + \frac{\partial(v \phi_i)}{\partial z} = \frac{X_{f,a}}{X_{f,i}} r_{ina} \quad (22)$$

The sum of specific generation rate of active and inactive bacteria causes biofilm volume to be expanded and contracted periodically [28]. As a result, the biofilm surface gains a convective velocity in respect to the fixed electrode surface of the cathode. The changes of this convection velocity along the biofilm thickness can be expressed as follows [28]:

$$\frac{\partial v}{\partial z} = (Yq - r_{res} - r_{ina}) + \left(\frac{X_{f,a}}{X_{f,i}} r_{ina}\right) \quad (23)$$

In addition to the total net specific growth rate of the bacteria, the biofilm thickness changes because of the detachment of bacteria from biofilm. Accordingly, the variation of biofilm thickness by time can be expressed by the following equation:

$$\frac{dL_f}{dt} = v(t, L_f) - b_{det}L_f \quad (24)$$

Initial and boundary conditions for solving the equation of 24 are listed below:

$$@ z = 0 , \quad v = 0 \quad (25)$$

$$@ t = 0 , \quad \phi_a = \phi_a^0 \quad (26)$$

Evidently, the decline rate and loss of the biofilm should not be greater than its growth rate to have of a stable biofilm. To this end, the minimum requirements for microbial growth must be determined carefully. In the present system, the substrate concentration and the electrical potential are the main factors influencing the microbial growth. Equations 27 and 28 determine the minimum substrate concentration and the electric potential to maintain a stable biofilm [10, 15]:

$$S_{a,min} = K_{sd} \frac{b_{ina} + b_{det}}{(Yq_{max} - b_{res}) - (b_{ina} + b_{det})} \quad (27)$$

$$\eta_{min} = \frac{RT}{F} \ln\left(\frac{b_{ina} + b_{det}}{(Yq_{max} - b_{res}) - (b_{ina} + b_{det})}\right) \quad (28)$$

2.7. Coulombic Efficiency

Coulombic efficiency (CE) of reverse microbial fuel cell can be defined as the ratio of the converted electrons to the final product to the supplied electrons to the system by the external current.

$$CE = \frac{J_s}{J_{e^-}} \quad (29)$$

$$J_{e^-} = j \frac{\tau}{F \gamma_1} \quad (30)$$

$$@ z = L_f, \quad J_s = D_{ED,f} \frac{dS_d}{dz} \quad (31)$$

2.8. Numerical Solution of the Model

Numerical techniques were used to solve the obtained differential equations in the model. Both of the differential equations (i.e. substrate concentration and the electric potential equation) are boundary and initial value problems which can be solved by two ways. The first method is finite difference and the second method is called the Shooting method. Since the equations are a combination of differential equations of boundary and initial value, it is appropriate to employ both techniques simultaneously. Figure 3 shows the solution flowchart of the model equations.

3. Results and Discussion

In this study, several important parameters of the MES system (e.g. the electrical potential, substrate concentration in biofilm, current density and biofilm thickness) have been monitored by time. In addition, the columbic efficiency as a function of substrate concentration has been investigated. Finally, validity of the model has been verified by comparing the obtained outputs with the related published experimental results. Numerical values of the physical coefficients and biochemical parameters of the model have been shown in table 2. The biochemical parameters were estimated for a pure microbial community of *Sporomusa ovata* growing on carbon dioxide [29]. The concentration of carbon dioxide in the catholyte solution was estimated by its solubility

in water using Henri's law in atmospheric pressure and ambient temperature which was calculated equal to $0.03 \text{ mmol cm}^{-3}$ [30].

Figures 4 and 5 illustrate the computed parameters of the cathodic chamber as a function of time and distance. As can be seen in figure 4-a, the electrical potential along the biofilm has slightly decreased. The induced potential difference in the biofilm causes electrons to transfer through the biofilm from the cathode to the biofilm/catholyte interface. The slight decrease of potential along the biofilm can be explained by its high electrical conductivity which means that the electron transfer should be controlled mainly by the liquid catholyte resistance in the system. In addition, electrical potential has increased by time because the current density has been reduced by the bacterial consumption and the potential of the cathode surface has increased according to the Ohm's law.

Variations of the substrate concentration in the biofilm have been shown in figure 4-b. The maximum substrate concentration has been obtained adjacent to the liquid boundary. Then, it has decreased continuously to about zero at the vicinity of the cathode. Since the conductivity of the biofilm is high enough to provide sufficient electrons, the decrease of substrate concentration in the biofilm can be explained by its diffusion and bioconversion rates.

The high concentration of substrate in the liquid boundary of the biofilm has a direct effect on accumulation of the active bacteria in this region. Figure 4-c shows the fraction of active bacteria along the biofilm. Clearly, the number of active microbes has increased towards the biofilm surface which is directly in contact with the substrate solution. In contrast, the number of active bacteria showed a drastic decrease near the cathode surface where the concentration of substrate went to zero. In fact, the inactive microorganisms near the cathode surface were only responsible for the conduction of electrons.

Biofilm thickness has been influenced by the net microbial growth and detachment rate. However, detachment has been ignored in this study because of the biofilm in RMFC systems have been reported to be very thin [3, 6]. As a result, a linear trend has been achieved for the variation of biofilm thickness by time (figure 5-a). As can be seen, the thickness of the biofilm reached to 25 microns from the initial value of zero, within 100 days. By the biofilm growth, the amounts of active bacteria within the biofilm would increase which in turn leads to an increase in the internal mass transfer resistance in the biofilm. The result obtained from these opposing effects causes the current density to decrease. In fact, with increasing distance from the cathode the substrate concentration and the number of active microorganisms increase resulting in the higher consumption of current density in that area.

The current density has decreased from 17.5 A.m^2 to 8.5 A.m^2 after 20 days as illustrated in figure 5-b. The required time for the current density to reach its final value is a function of the surface potential of the cathode and the substrate concentration in the bulk liquid.

Besides the current density, coulombic efficiency is also an important parameter for evaluating and comparing the performance of the reverse microbial fuel cell. Coulombic efficiency indicates the ratio of the electrons participated in acetate synthesis to electrons consuming as the current density. Under the proposed conditions of the model, the coulombic efficiency was obtained equal to 59%. This value was calculated by dividing the output product molar flux from the surface of biofilm (in $\text{mmol acetate.cm}^{-2}.\text{day}$) to the electron consumption flux as current density in the same unit (eq.29).

However, according to figures 4-a, 4-b and 5-b, when the substrate concentration has the maximum value, current density and electric potential are the lowest. In fact, current density and

electric potential play a limiting role for acetate production in the dual limitation condition which was described by equations 2 and 3. This effect will be studied in detail in the following section.

3.1. Investigation of the Dual Limiting Effect

Generally, there are three limiting factors affecting the current density consumption in the reverse microbial fuel cells [31, 33]:

- Substrate concentration
- Potential of the cathode surface
- Changes of pH within biofilm and electrolyte solution

In this study, the changes of pH in the biofilm and electrolyte solution have been assumed to be negligible and only the first two factors were studied. This investigation was performed using the substrate utilization equation (Eq. 3), which is a dual limitation equation. In this equation, the substrate consumption rate has been expressed as a function of both the substrate concentration and the potential of cathode surface which can restrict the current density consumption and efficiency of the acetate production. The range of variation for both concentration and potential limiting conditions has been shown in table 3. The performance of the modeled MES system has been evaluated in terms of current density and Coloumbic efficiency for each range.

Figure 6-a shows the coloumbic efficiency versus substrate concentration in the bulk liquid which has been changed from 10 to 75%. The results indicated that increasing the substrate concentration in catholyte caused a significant decrease in the cell yield (coloumbic efficiency). The coloumbic efficiency reached to its maximum value at 75% for the minimum catholyte substrate concentration equal to $0.025 \text{ mmol.cm}^{-3}$. In fact, the maximum coloumbic efficiency determines the maximum capacity of active microbes in catalysis of the acetate production

reaction from carbon dioxide. As mentioned before, the coulombic efficiency is the ratio of output product flux from the biofilm to the electron flux consumption as the current density. Therefore, with the minimum amount of substrate at the saturated potential condition (state 1), maximum amounts of product yield (e.g. acetate) will be obtained because a higher portion of the substrate can be oxidized by the chemical synthesis available electrons and will be converted into the product at the lower concentrations.

Variations of the current density and biofilm thickness for the state (1) have been demonstrated in Figures 6-b and 6-c. The similarity of biofilm thickness and current density profiles can be explained through their direct relationships as described in equation 14 before. The results for the Nernst- Monod term of equation (3), which is equal to half the maximum value of E_{KA} potential has been shown in figure 7-a (state 2). Apparently, the current density has been affected just by a small range of cathodic potential from -0.1V to 0.1V around E_{KA} . In other words, in the electrically conductive biofilm which has been described by the Nernst – Monod equation, the variation of potential influences the current density in only a narrow range and beyond this interval it is saturated. The trend of current density by the cathode potential has been shown in figure 7-b. Evidently, the current density has decreased in constant cathode surface potential and then declined sharply. The reason may be described by the fact that the process has been controlled by the external mass transfer resistances and the cathode surface potential will not cause any significant changes in the film density in such criteria.

On the basis of the above, the minimum potential ($\eta = E_{KA} - V_{cath}$) to have a stable biofilm with respect to the reference value can be calculated from equation 28 which is equal to 1.13 V (for -0.682 V as potential of the cathode). As shown in to figure 7-b, Coloumbic efficiency

increases with an increase in the cathode surface voltage and in the potential of -0.3 V it has the highest value equal to 55%.

3.2. Investigation of the Validity of the Obtained Model by Experimental Results

To examine the validity of the assumptions made to the model, obtained results were compared to experimental reports of similar conditions. We run the model at the same conditions as Lovely et al. have investigated the acetate production from carbon dioxide in a R-MFC system [3, 6]. The obtained coulombic efficiency of the model by time has been shown in figure 8-a for *Sporomusa ovata* and carbon dioxide as the carbon source for microbial community, which is about 51% constant.

However, in this study it was assumed that the only product of the process was acetate whereas in the empirical MES, it has been reported to have at least two final products (e.g. acetate and 2-oxobutyrate). As shown in figure 8-b, coulombic efficiency of 2-Oxobutyrate and acetate are about 10% and 50% respectively at the beginning of the process. These values are almost constant until the fourth day and after that, the yield of acetate production decreases while that of 2-Oxobutyrate goes up. However, the summation of coulombic efficiencies of both products should be considered for the comparison with the model results which is initially around 60% and decreases to about 50% after the fourth day. Evidently, there is a good consistency between the model and experimental results in this case especially after four days which could be considered as a sign for the validity of the proposed model.

4. Conclusions

In this work, bio-electrosynthesis of acetate from CO₂ (substrate) and H₂O has been modeled in a reverse microbial fuel cell to predict important cathodic parameters such as substrate

concentration profile, electrical potential, current density and biofilm thickness. The effect of substrate concentration and cathodic potential on the Coulombic efficiency has been studied as well. It was observed that the increase of the substrate concentration had a negative effect on Coulombic efficiency at constant potential while at the constant substrate concentration Coulombic efficiency went up by increasing the cathodic potential. Correspondingly, the maximum Coulombic efficiency was calculated about %75 in the substrate concentration of $0.025 \text{ mmol cm}^{-3}$ and %55 in the surface cathodic voltage of -0.3 V . At last, the obtained results for the acetate production were compared with experimental findings which showed a good agreement and validity of the model assumptions was verified.

5. References

- [1] A. ElMekawy, H. M. Hegab, K. Vanbroekhoven, D. Pant, Techno-productive potential of photosynthetic microbial fuel cells through different configurations, *Renewable and Sustainable Energy Reviews*, 39 (2014) 617-627.
- [2] D. R. Lovley, Powering microbes with electricity: direct electron transfer from electrodes to microbes, *J. Environmental Microbiology Reports*. 3(2011) 27-35.
- [3] P.K. Nevin, L.T. Woodard, E.A. Franks, M.Z. Summers, D.R.Lovley, Microbial Electrosynthesis: Feeding Microbes Electricity to Convert Carbon Dioxide and Water to Multicarbon Extracellular Organic Compounds, *J. mBio*. 1(2010) 3-10.
- [4] K. Rabaey, A. R. René, Microbial electrosynthesis revisiting the electrical route for microbial production, *J. Applied and Industrial Microbiology*. 8 (2010) 706-716.
- [5] M.H. Osman, A.A. Shah, F.C. Walsh, Recent progress and continuing challenges in bio-fuel cells. Part I: Enzymatic cells, *J. Biosensors and Bioelectronics*. 26(2011) vol. 3087–3102.

- [6] P.N. Kelly, A.S. Hensley, E.A. Franks, M.Z. Summers, O. Jianhong, L.T. Woodard, L.O.Snoeyenbos-West, R.D. Lovley, Electrosynthesis of Organic Compounds from Carbon Dioxide Is Catalyzed by a Diversity of Acetogenic Microorganisms, *J. Applied and Environmental Microbiology*. 77(2011) 2882–2886.
- [7] S. Srikanth, M. Maesen, X. Dominguez-Benetton, K. Vanbroekhoven, D. Pant, Enzymatic electrosynthesis of formate through CO₂ sequestration/reduction in a bioelectrochemical system (BES), *Bioresource technology*. 165(2014) 350-354.
- [8] P. Clauwaert, R. Tole[^] do, D. van der Ha, R. Crab, W. Verstraete, H. Hu, K. M. Udert, K. Rabaey, Combining biocatalyzed electrolysis with anaerobic Digestion, *J. Water Science & Technology*. 57(2008) 575-579
- [9] X. Dominguez-Benetton, S. Srikanth, Y. Satyawali, K. Vanbroekhoven, D. Pant, Enzymatic electrosynthesis: An overview on the progress in enzyme-electrodes for the production of electricity, fuels and chemicals, *J Microb Biochem Technol*. (2013) S, 6, 2.
- [10] B.E. Rittmann, P.L.McCarty, *Environmental biotechnology: principles and applications*, first ed., McGraw-Hill, New York, 2001.
- [11] Z. Du, H. Li, T. Gu, A state of the art review on microbial fuel cells: a promising technology for wastewater treatment and bioenergy, *J.Biotechnology Advances*. 25(2007) 464–482.
- [12] W. Bae, B.E. Rittmann, Responses of intracellular cofactors to single and dual substrate limitations, *J. Biotechnology and Bioengineering*. 49(1996) 690–699.
- [13] W. Bae, B.E. Rittmann, A structured model of dual-limitation kinetics, *J. Biotechnology and Bioengineering*. 49(1996) 683–689.

- [14] M. Sharma, N. Aryal, P. M. Sarma, K. Vanbroekhoven, B. Lal, X. Dominguez Benetton, D. Pant, Bioelectrocatalyzed reduction of acetic and butyric acids via direct electron transfer using a mixed culture of sulfate-reducers drives electrosynthesis of alcohols and acetone, *Chemical Communications*. 49(2013) 6495-6497
- [15] K.A. Marcus, C.I. Torres, B.E. Rittmann, Conduction based modeling of the biofilm anode of a microbial fuel cell, *J. Biotechnology and Bioengineering*. 98(2007) 1171–1182.
- [16] H. Horn, D.C. Hempel, Modeling mass transfer and substrate utilization in the boundary layer of biofilm system, *J. Water Science and Technology*. 37 (1998) 139-147.
- [17] K.A. Marcus, C.I. Torres, B.E. Rittmann, Conduction based modeling of the biofilm anode of a microbial fuel cell, *J. Biotechnology and Bioengineering*. 98(2007) 1171–1182.
- [18] O. Wanner, H.J. Eberl, E. Morgenroth, D.R. Noguera, C. Picioreanu, B.E. Rittmann, M.V. Loosdrecht, *Mathematical modeling of biofilms*, first ed., IWA, UK, 2006.
- [19] K. Rasmussen, Z. Lewandowski, Microelectrode measurements of local mass transport rates in heterogeneous biofilms, *J. Biotechnology and Bioengineering*. 59(1998) 302-309.
- [20] H. Horn, D.C. Hempel, Mass transfer coefficients for an autotrophic and a heterotrophic biofilm system, *J. Water Science and Technology*. 32(1995) 199-204.
- [21] R.B. Bird, W.E. Stewart, E.N. Lightfoot, *Transport phenomena*, second ed., John Wiley & Sons Inc, New York, 2003.
- [22] H. Beyenal, Z. Lewandowski, Internal and external mass transfer in biofilms grown at various flow velocities, *J. Biotechnology Progress*. 66(2002) 55-61.
- [23] H. Horn, D.C. Hempel, Substrate utilization and mass transfer in an autotrophic biofilm system: experimental results and numerical simulation, *J. Biotechnology and Bioengineering*. 53(1997) 363-371.

- [24] D.M. Bernardi, M.W. Verbrugge, Mathematical-model of a gas-diffusion electrode bonded to a polymer electrolyte, *J. AIChE.* 37(1991) 1151-1163.
- [25] I.U. Hwanga, H.N. Yua, S.S.Kima, D. Gil Lee, Bipolar plate made of carbon fiber epoxy composite for polymer electrolyte membrane fuel cells, *J.Power Sources.* 184(2008) 90-94.
- [26] J.R. Kim, S. Cheng, S.E. Oh, B.E. Logan, Power generation using different cation, anion and ultrafiltration membranes in microbial fuel cells, *J. Environmental Science and Technology.* 41 (2007) 1004-1009.
- [27] A.T.Heijne, H.V.M. Hamelers, V.D. Wilde, R.R. Rozendal, C.J.N. Buisman, Ferric iron reduction as an alternative for platinum-based cathodes in microbial fuel cell, *J. Environmental Science and Technology.* 40(2006) 5200-5205.
- [28] O. Wanner, W. Gujer, A multispecies biofilm model, *J. Biotechnology and Bioengineering.* 28 (1986) 314–328.
- [29] C. Picioreanu, I.M. Headc, K.P. Katuri, M.C.M. Van Loosdrecht, A computational model for biofilm-based microbial fuel cells, *J. Water Research.* 41(2007) 2921–2940.
- [30] Perry, *Chemical engineering's handbook*, eighth ed., McGraw-Hill Professional, New York, 2007.
- [31] C.I. Torres, K.A. Marcus, P. Parameswaran, B.E. Rittmann, Kinetic experiments for evaluating the Nernst-Monod model for anode-respiring bacteria (ARB) in a biofilm anode, *J. Environmental Science and Technology.* 42(2008) 6593–6597.
- [32] D.R. Bond, D.R. Lovley, Electricity production by *geobacter sulfurreducens* attached to electrodes, *J. Applied and Environmental Microbiology.* 69(2003) 1548–1555.

[33] C.I. Torres, K.A. Marcus, B.E. Rittmann, Proton transport inside the biofilm limits electrical current generation by anode-respiring bacteria, *J. Biotechnology and Bioengineering*. 100(2008) 872-881.

Figure Captions:

- Figure 1: Possible routes of electron consumption in a R-MFC system
- Figure 2: A simple profile of the biofilm attached to the cathode and the relevant concentration boundary layer
- Figure 3: Flowchart of the model
- Figure 4: The computed parameters as a function of distance: a) electrical potential, b) substrate concentration and c) volume fraction of active microbes in the biofilm
- Figure 5: The computed parameters as a function of time a) biofilm thickness and b) current density.
- Figure 6: The calculated parameters at saturated potential condition versus substrate concentration in the catholyte (state 1): a) Coloumbic efficiency, b) current density and c) biofilm thickness
- Figure 7: The calculated parameters at saturated substrate concentration condition versus cathode potential (state 2): a) Nernst - Monod and b) changes of current density and Coloumbic efficiency
- Figure 8: comparison of the model results with the relevant experimental data, a) model results, and b) experimental data.

Table Captions:

- Table 1: Employed terms for the model parameters and their units
- Table 2: Numerical values of the model parameters
- Table 3: Range of variations in cathode surface potential and catholyte substrate concentration

Table 1: Employed terms for the model parameters and their units

Parameter	description	Units
q	Substrate consumption specific rate	$\text{mmol S.mg}^{-1}.\text{day}^{-1}$
q_{\max}	Maximum substrate consumption specific rate	$\text{mmol S.mg}^{-1}.\text{day}^{-1}$
ϕ_a	Volume fraction of active bacteria	Dimensionless
S_d	Electron donor concentration	mmol.cm^{-3}
K_{sd}	Monod half-saturation coefficient for electron donor	mmol.cm^{-3}
S_a	Electron acceptor concentration	mmol.cm^{-3}
K_{sa}	Monod half-saturation coefficient for electron acceptor	mmol.cm^{-3}
F	Faraday's constant	C.mol^{-1}
R	Universal gases constant	$\text{J.mol}^{-1}.\text{K}^{-1}$
T	Process temperature	K
η	Electrical potential in the biofilm	V
r_{res}	Specific rate of active bacteria self-oxidation	day^{-1}
b_{res}	Self-oxidation constant	day^{-1}
r_{ina}	Inactivated rate of active bacteria	day^{-1}
b_{ina}	Inactivated constant	day^{-1}
$D_{ED,f}$	Corrected diffusion coefficient substrate in the biofilm	$\text{cm}^2.\text{day}^{-1}$
Z	Coordinate in the biofilm (perpendicular to the cathode electrode surface)	cm
$X_{f,a}$	Active biomass density	mg X.cm^{-3}
L_f	Biofilm thickness	cm
$D_{ED,l}$	Diffusion coefficient of substrate in the water	$\text{cm}^2.\text{day}^{-1}$
L	Concentration boundary layer thickness	cm
$S_{a,\text{bulk}}$	Substrate concentration in the catholyte	mmol.cm^{-3}
$S_{a,\text{surface}}$	Substrate concentration on the biofilm surface	mmol.cm^{-3}
Sh	Sherwood number	Dimensionless
Re	Reynolds number	Dimensionless
Sc	Schmidt number	Dimensionless
d_h	Hydrodynamic diameter	cm
L_e	Electrode length	cm
k_l	External mass transfer coefficient	cm.day^{-1}
u	Average rate	cm.day^{-1}
ν	Kinematic viscosity	$\text{cm}^2.\text{day}^{-1}$

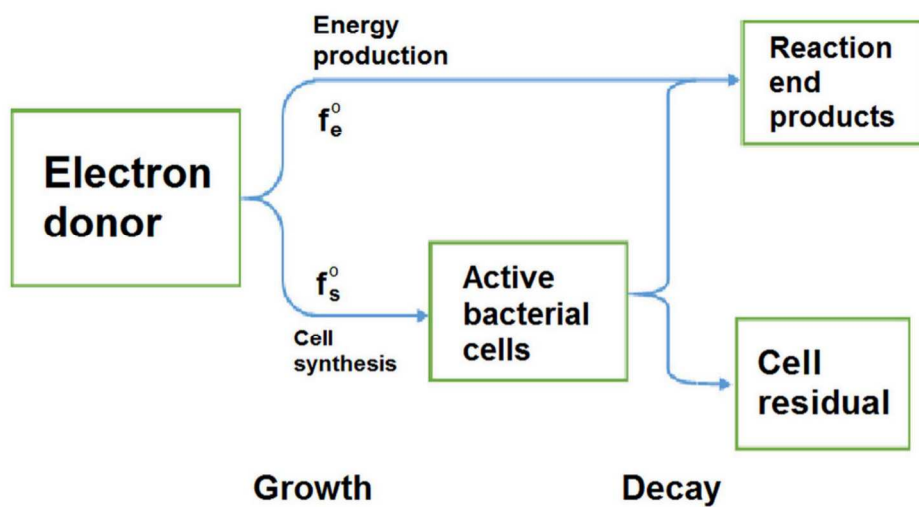
u_x	average flow rate of substrate	$\text{cm}\cdot\text{day}^{-1}$
J_s	Substrate molar flux passing through the surface of the biofilm	$\text{mmol}\cdot\text{cm}^{-2}\cdot\text{day}^{-1}$
$V_{c,b}$	Cathode chamber volume	cm^3
A_s	Cathode electrode area	cm^2
$S_{a,bulk}^0$	Initial substrate concentration in the catholyte	$\text{mmol}\cdot\text{cm}^{-3}$
$S_{a,in}$	Inlet substrate concentration	$\text{mmol}\cdot\text{cm}^{-3}$
j	Current density	$\text{mA}\cdot\text{cm}^{-2}$
k_{bio}	Electrical conductivity coefficient	$\text{mS}\cdot\text{cm}^{-1}$
γ_1	Electron equal production	$\text{mmole}^{-}\cdot\text{mmol}$
γ_2	Electron equal active biomass	$\text{mmole}^{-}\cdot\text{mmolX}$
f_e^o	Fraction electrons of energy generation	Dimensionless
τ	Conversion of second to day	$86400\text{ s}\cdot\text{day}^{-1}$
$V_{cathode}$	Electrical potential of cathode surface	volt
$\sum R$	Sum of the ohmic's resistances and external electrical resistances	$\text{K}\Omega$
d	Distance of electrode from membrane	cm
K_{sol}	Electrical conductivity coefficient of electrolyte	$\text{mS}\cdot\text{cm}^{-1}$
ΔV_{ohm}	Voltage losses because of ohmic's resistances	volt
v	Convective rate into the biofilm	$\text{cm}\cdot\text{day}^{-1}$
Y	Real microbial yield	$\text{mgX}\cdot\text{mmol sub}^{-1}$
t	time	Day
ϕ_i	Volume fraction of inactive bacteria	Dimensionless
$X_{f,i}$	Inactive biomass density	$\text{mg}\cdot\text{cm}^{-3}$
b_{det}	Detachment constant	day^{-1}
$S_{a,min}$	Minimum concentration of substrate	$\text{mg}\cdot\text{cm}^{-3}$
η_{min}	Minimum potential	Volt
CE	Coloumbic efficiency	Dimensionless
J_e^{-}	Consuming electron flux as current density	$\text{mmol}\cdot\text{cm}^{-2}\cdot\text{day}^{-1}$
J_s	Output product flux from the biofilm	$\text{mmol}\cdot\text{cm}^{-2}\cdot\text{day}^{-1}$

Table 2: numerical values of the model parameters

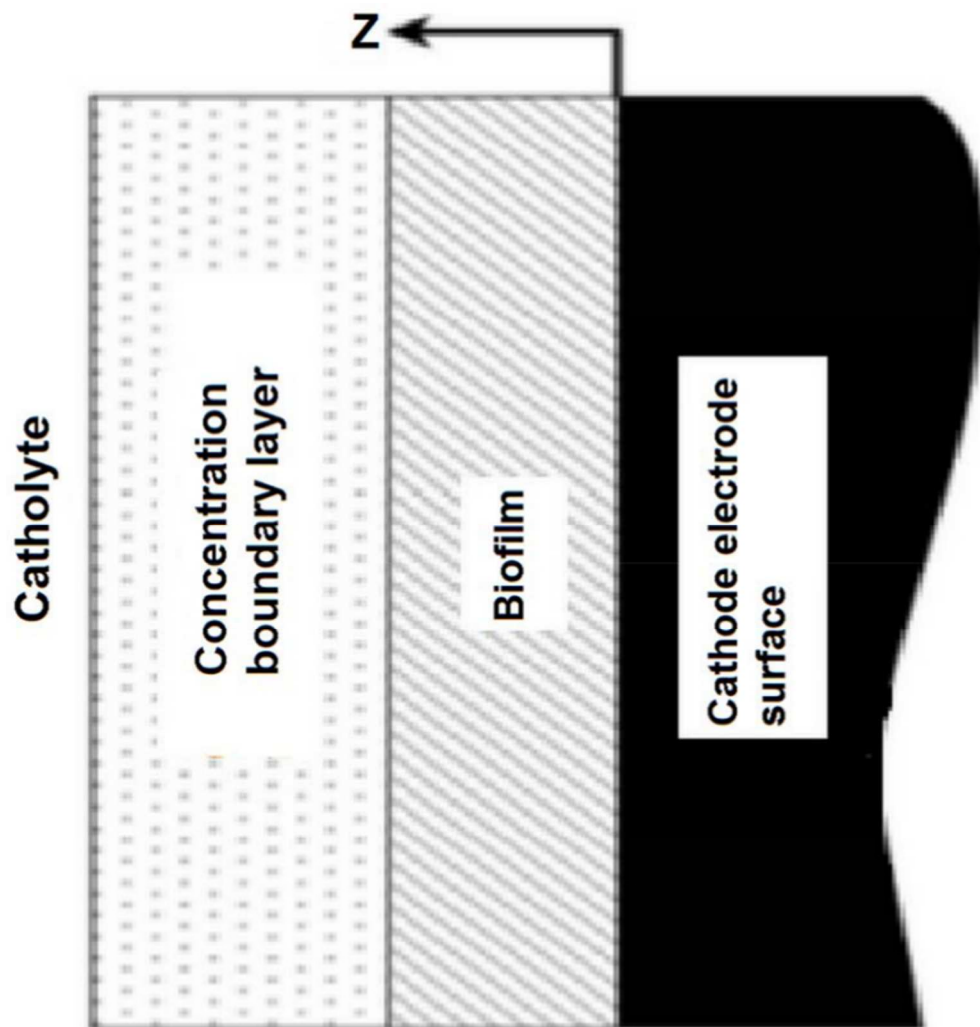
Symbol	Amount	Unit	Reference	Symbol	Amount	Unit	reference
K_{sa}	$2 \cdot 10^{-5}$	$Mmol.cm^{-3}$	[Picioreanu et al., 2007]	L	0.01	cm	[Wanner et al., 2006]
q_{max}	0.2	$mmol.mg^{-1}.day^{-1}$	[Picioreanu et al., 2007]	E_{KA}	0.448	V	[Torres et al., 2008a]
$D_{ED,l}$	1.1559	$Cm^2.day^{-1}$	[Green and Perry, 2007]	$X_{f,a}, X_{f,i}$	50	$mg X.cm^{-3}$	[Picioreanu et al., 2007]
$D_{ED,f}$	0.9247	$Cm^2.day^{-1}$	[Wanner et al., 2006]	Y	6.8509	$mgX.mmol^{-1}$	[Picioreanu et al., 2007]
γ_1	8	$mmole^{-1}.mmol$	[Rittmann and McCarty, 2001]	f_c^0	0.8	dimensionless	[Rittmann and McCarty, 2001]
γ_2	1.74	$mmole^{-1}.mmolX$	[Rittmann and McCarty, 2001]	k_{bio}	0.5	$mS.cm^{-1}$	[Torres et al., 2008a]
b_{res}	0.05	Day^{-1}	[Rittmann and McCarty, 2001]	V_{cath}	-0.28	V	[Bond and Lovley, 2003]
b_{ina}	0.05	Day^{-1}	[Rittmann and McCarty, 2001]	T	303.15	K	
F	96485	$C.mol^{-1}$		R	8.3145	$J.mol^{-1}.K^{-1}$	

Table 3: Range of variations in cathode surface potential and catholyte substrate concentration

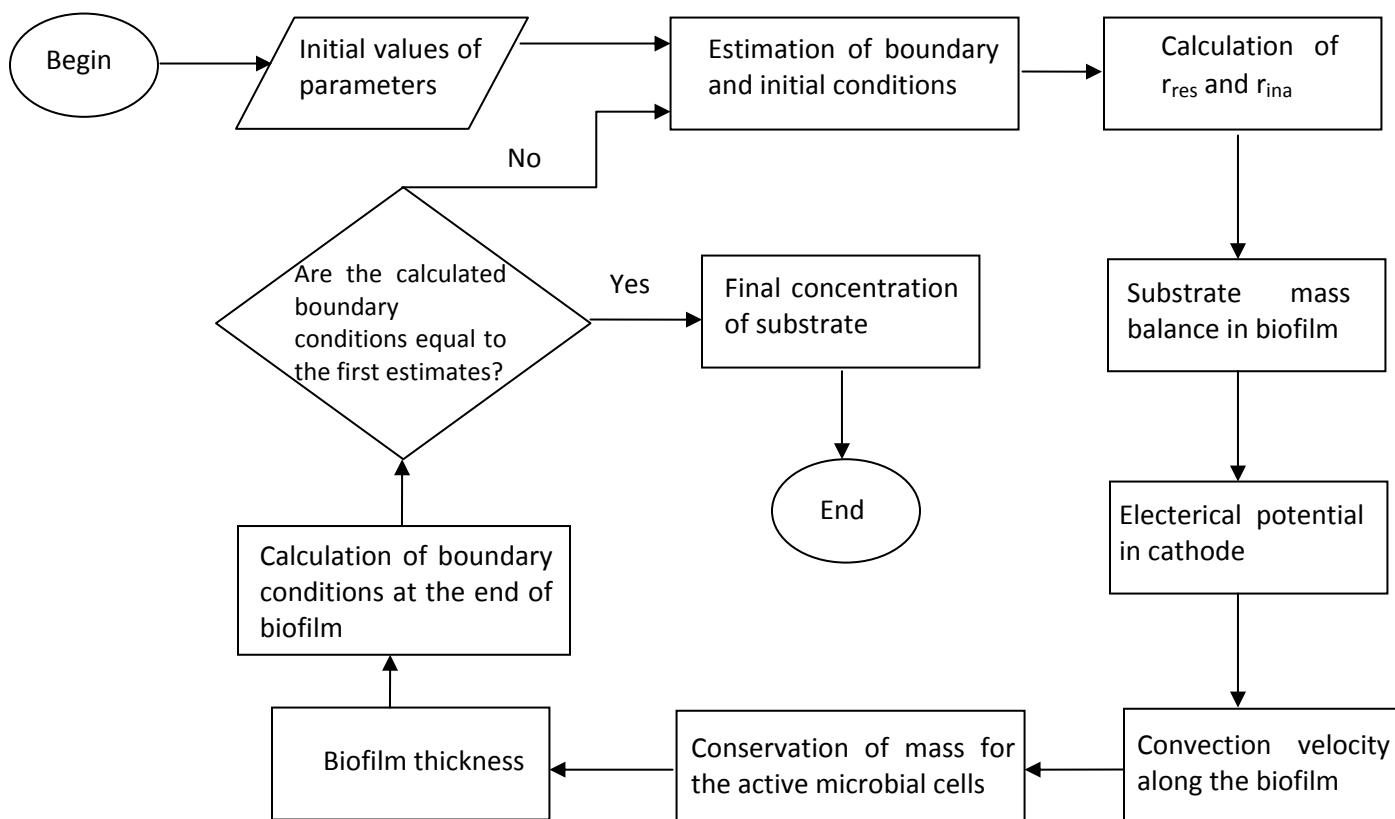
Limitating factors	State 1 (saturated potential)	State 2 (saturated substrate concentration)
Cathode surface potential (volt)	-0.4	-0.5to -0.3
Substrate concentration in bulk liquid (mmol.cm ⁻³)	0.025 to 0.05	0.03

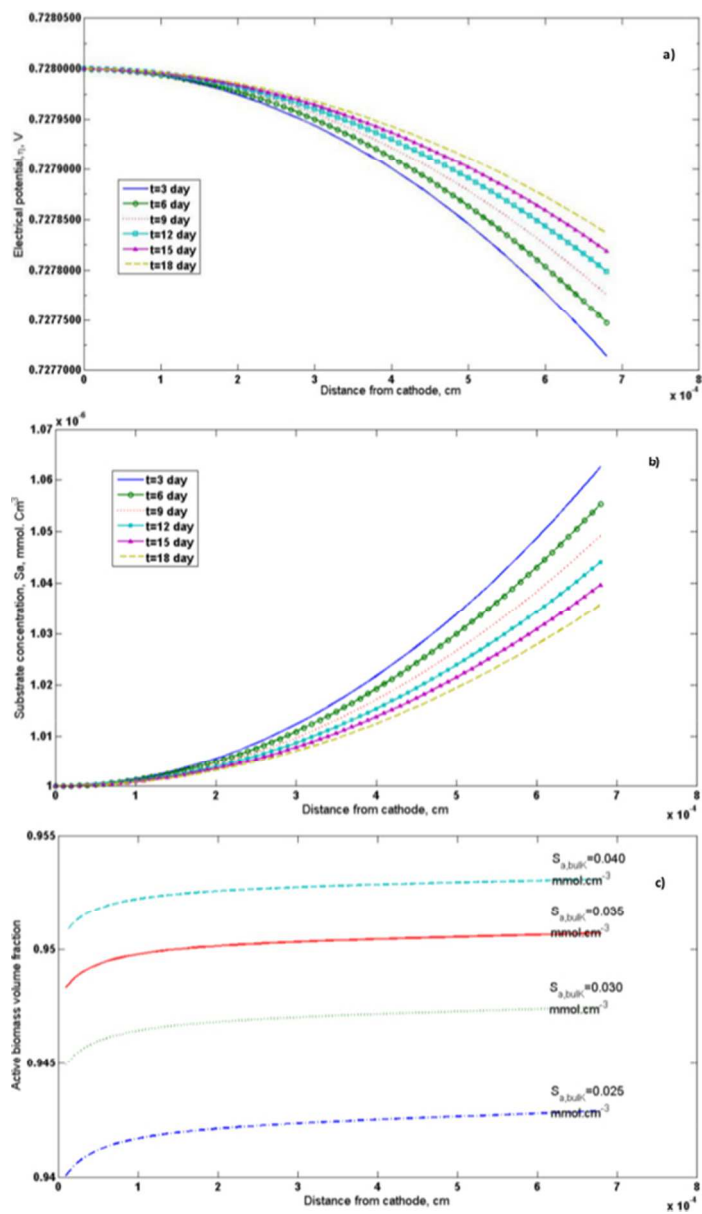


131x79mm (270 x 270 DPI)

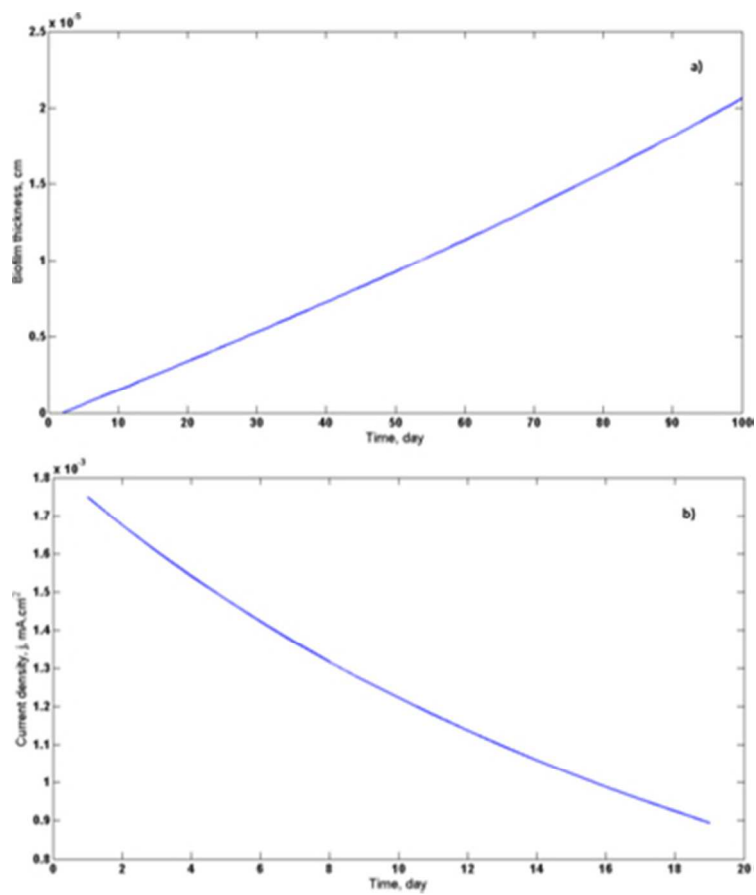


65x68mm (300 x 300 DPI)

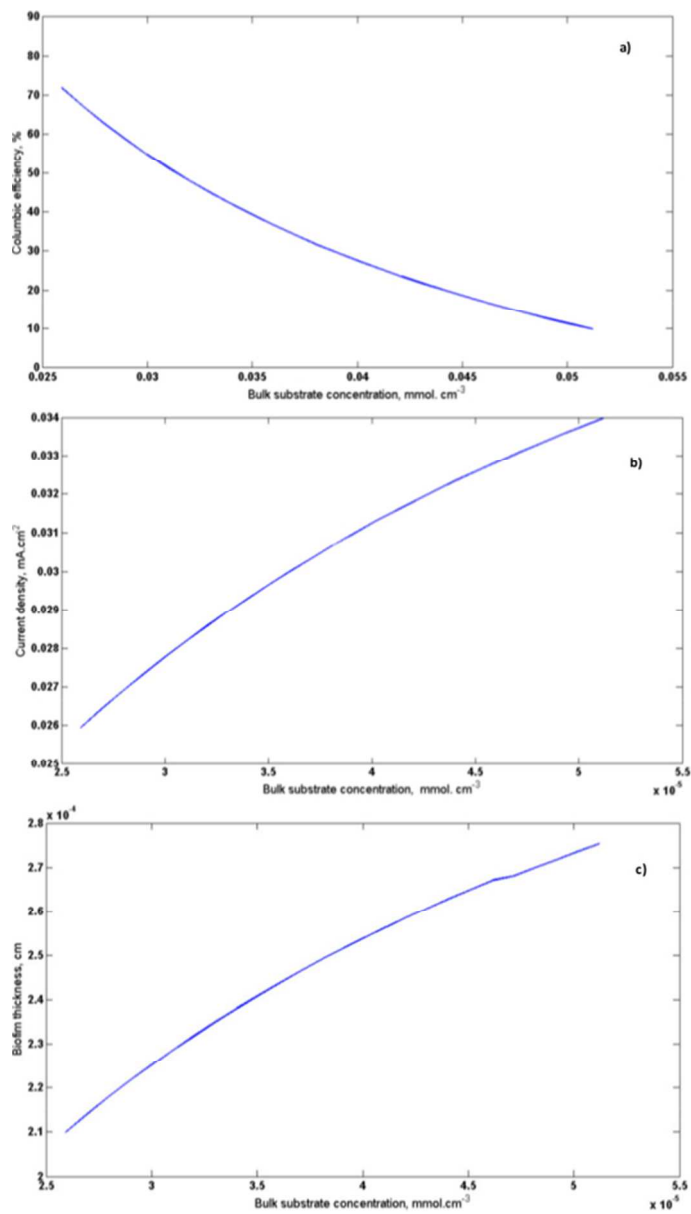




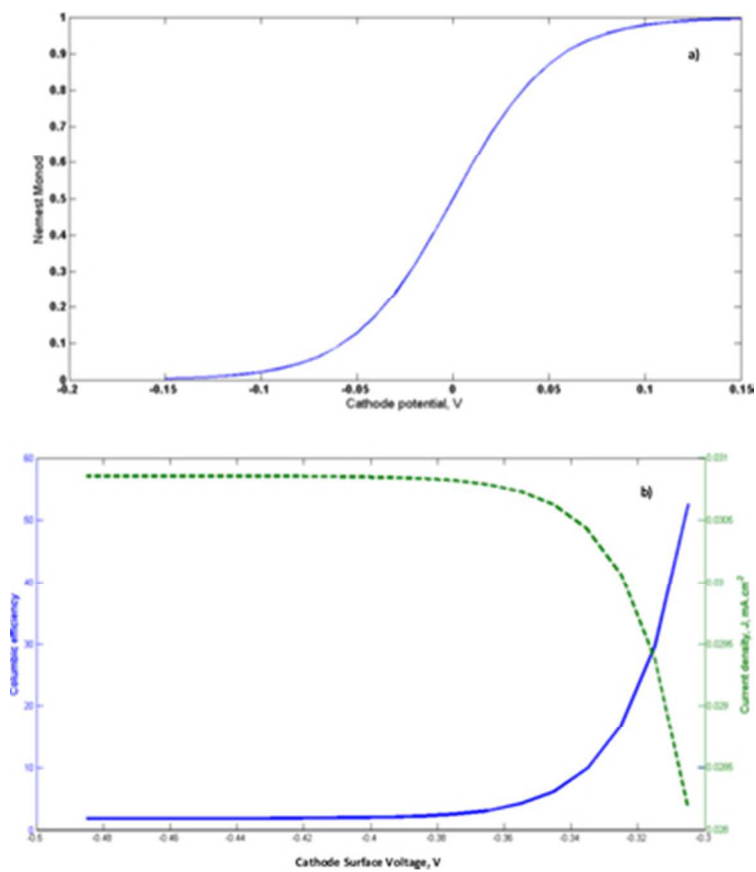
45x79mm (300 x 300 DPI)



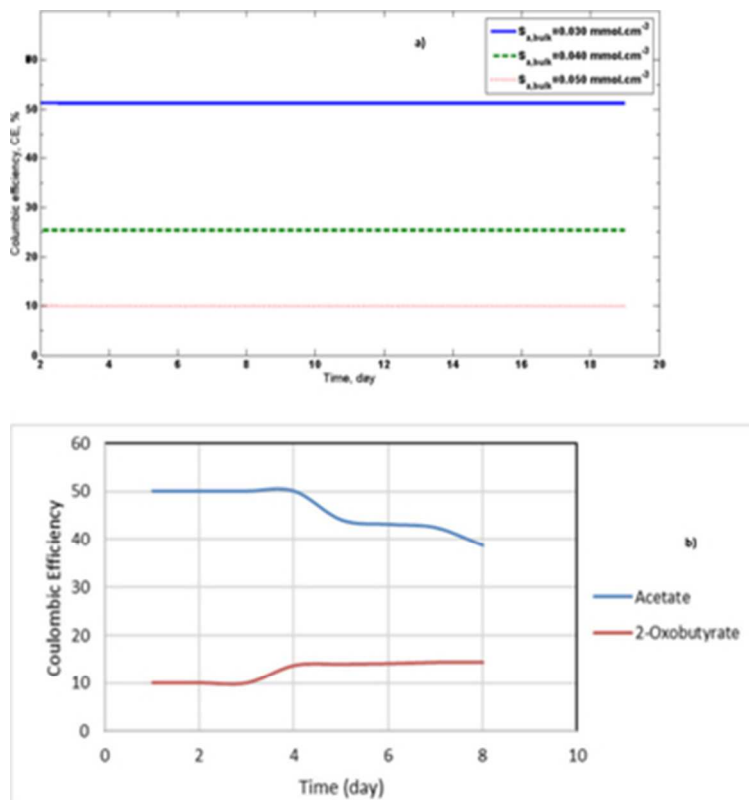
31x37mm (300 x 300 DPI)



44x78mm (300 x 300 DPI)



31x36mm (300 x 300 DPI)



31x33mm (300 x 300 DPI)

Bio-electrosynthesis of organic compounds (citrate) in a reverse microbial fuel cell:

